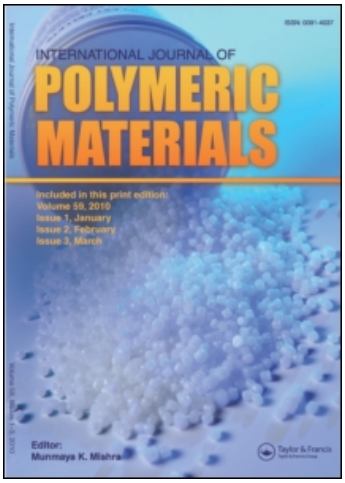

International Journal of Polymeric Materials
Publication details, including instructions for authors and subscription information:
http://www.informaworld.com/smpp/title~content=t713647664

Flow Stability of Polymer Melts in Simple Shear

L. A. Faitelson[a]
[a] Institute of Polymer Mechanics, Latvian SSR Academy of Sciences, Riga, U.S.S.R.

To cite this Article Faitelson, L. A.(1982) 'Flow Stability of Polymer Melts in Simple Shear', International Journal of Polymeric Materials, 9: 3, 153 — 166
To link to this Article: DOI: 10.1080/00914038208077977
URL: http://dx.doi.org/10.1080/00914038208077977

Inter. J. Polymeric Mater., 1982, Vol. 9, pp. 153–166
0091–4037/82/0903–0153 $06.50/0

Printed in Great Britain

Flow Stability of Polymer Melts in Simple Shear†

L. A. FAITELSON
Institute of Polymer Mechanics, Latvian SSR Academy of Sciences, Riga, U.S.S.R.

(*Received June 4, 1981*)

It is shown that the strain rates leading to shear flow instability in the form of polymer melts and solutions squeezing out of the working gap, occurrence of visible eddies on the free surfaces of test samples in cone-and-plate rheometers, $\lim_{\omega \to 0} G'(\omega, \dot{\gamma}_0) < 0$ at parallel superposition of steady and oscillatory shears, and break of practically monodisperse linear polymers forced through a nozzle, are determined by the second shear rate derivative of the elastic energy accumulated at a steady shear flow.

For polydisperse polymers, stable and instable flow conditions are associated with polymer segregation according to molecular weights ($M > M_c$) into clusters which migrate toward the nozzle axis, if incipient instability originates inside the nozzle. Instability originating at the nozzle inlet is analysed, consideration being given to pre-stationary flow conditions. Clusters are treated as dissipative structures according to Prigozhin.

1. IN A HOMOGENEOUS SHEAR RATE AND STRESS FIELD

When this is achieved at small angles between a cone and plate in the cone-and-plate instruments, starting from some critical shear rate $\dot{\gamma}^*$ a steady laminar melt flow fails to be attained, the material is squeezed out of the working gap, double meniscus is formed along the contour, and melt balls occur along the periphery. We have found[1] that γ^* is determined by the zero value of the second shear rate derivative of the accumulated energy, $d^2E_e/d\dot{\gamma}^2$ (at its transition form positive to negative values), which separates a stable stationary flow region ($d^2E_e/d\dot{\gamma}^2 > 0$), from an instable region ($d^2E_e/d\dot{\gamma}^2 < 0$).

If the accumulated steady flow strain is $\gamma_e = P_{w1}/2\sigma_{12} = c\dot{\gamma}^k$, where $P_{w1} = \sigma_{11} - \sigma_{22}$ is the first normal stress difference, σ_{12} are shear stress, and c and k

† Presented at the XI All-Union Symposium on Rheology of Polymers, May 12–16, 1980 in Suzdal (U.S.S.R.).

are constants, then

$$d^2E_e/d\dot{\gamma}^2 = k\frac{d(P_{w1}/2\dot{\gamma})}{d\dot{\gamma}}. \tag{1}$$

In a general case,

$$dE_e/d\dot{\gamma} = \sigma_{12}\, d\gamma_e/d\dot{\gamma} = 0.5dP_{w1}/d\dot{\gamma} - (P_{w1}/2\sigma_{12})(d\sigma_{12}/d\dot{\gamma}). \tag{2}$$

It is evident that $P_{w1}/2\sigma_{12}$ characterises the strain accumulated in the simple shear flow regime rather than elastic recovery $\gamma > \gamma_e$ which is determined in the unsteady regime.

Figure 1 shows $dE_e/d\dot{\gamma}$ for high-density polyethylene investigated in Ref. 2. The agreement between the prediction and experimental curves is seen to be quite satisfactory. Single arrows show rates $\dot{\gamma}$ at which the melt is squeezed out of the gap, as well as rates $\dot{\gamma}$ (at the top) at which $d^2E_e/d\dot{\gamma}^2 = 0$ as calculated using Eq. (2). Double arrows show rates $\dot{\gamma}$ corresponding to $d^2E_e/d\dot{\gamma}^2 = 0$ calculated using Eq. (1). Both melts and particularly melt B can be seen for $P_{w1}/2\sigma_{12} \neq c\dot{\gamma}^k$; calculations per Eq. (2) hold true as well.

As may be seen from Figures 2 and 3, the stability criterion calculated using

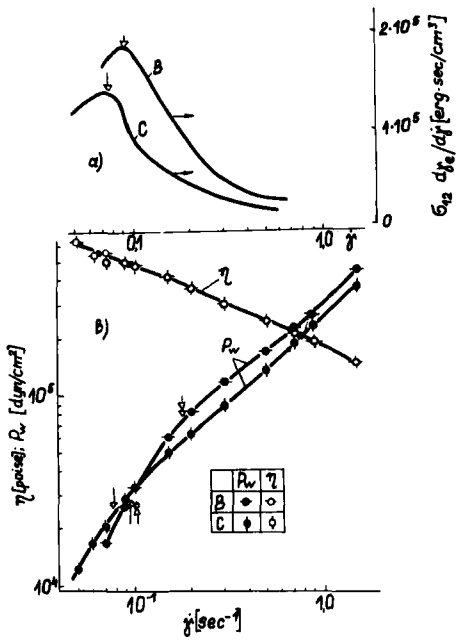

FIGURE 1 High-density polyethylene[2], a) $\sigma_{12}\, d\gamma_e/d\dot{\gamma}$ *vs.* $\dot{\gamma}$ relation $\downarrow$ – max $\sigma_{12}\, d/\gamma_e/d\dot{\gamma}$; b) material functions $\eta - \gamma$ and $P_{w1} - \dot{\gamma}$. $\downarrow$, test sample squeezing out of the working gap of the rheometer; $d^2E_e/d\dot{\gamma}^2 = 0$ according to Eq. (2); $\downarrow$, $d^2E_e/d\dot{\gamma}^2 = 0$ calculated according to Eq. (1).

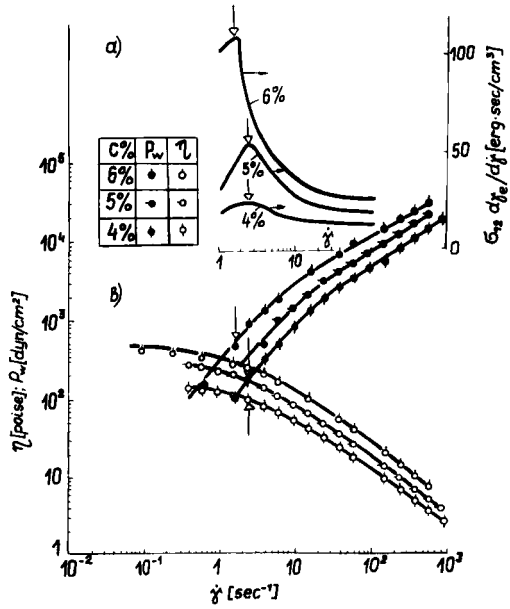

FIGURE 2 Aqueous polyacrylamide solutions.[4] a) $\sigma_{12}\, d\gamma_e/d\dot{\gamma}$ *vs.* $\dot{\gamma}$ relations. ↓, max $\sigma_{12}\, d\gamma_e/d\dot{\gamma}$; b) material functions $\eta - \dot{\gamma}$ and $P_{w1} - \dot{\gamma}$. ↓, lowest shear rates for observation of vortices.

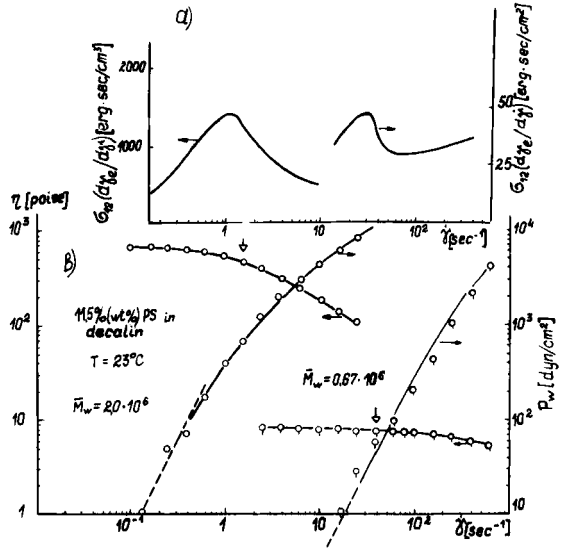

FIGURE 3 Two polystyrene solutions in decalin.[3] a) $\sigma_{12}\, d\gamma_e/d\dot{\gamma}$ *vs.* $\dot{\gamma}$ relation. ↓, max $\sigma_{12}\, d\gamma_e/d\dot{\gamma}$; b) material functions $\eta - \dot{\gamma}$ and $P_{w1} - \dot{\gamma}$. ↓, lowest shear rates for observation of vortices.

Eq. (2) characterises the eddy flow[3,4] setting in aqueous polyacrylamide solutions and polystyrene solutions in decalin, respectively, under the same deformation conditions. The method used in Refs 3 and 4 to predict eddy flows seems to be artificial and rather subjective, as evidenced by Figure 4 showing conventional coordinate calculations per Ref. 4. It is of interest to note that stationary flow rates $\dot{\gamma}_0$ which, when superimposed as periodic low-amplitude shear with frequency ω in the flow direction, may possibly induce negative values for the real part of the complex shear modulus $G'(\omega, \dot{\gamma}_0)$, are determined according to Refs 5 and 6 by the following criterion:

$$d(P_{w1}/2\dot{\gamma})/d\dot{\gamma} < 0. \tag{3}$$

This criterion holds true for particular cases when $P_{w1}/2\sigma_{12} \sim \dot{\gamma}^k$. As it follows from the analysis presented in Refs 7 and 8, a general case is characterised by the criterion $d^2E_e/d\dot{\gamma}^2 < 0$, with $dE_e/d\dot{\gamma}$ determined using Eq. (2).

Reference 7 shows that criterion (3) is effective for:

1) Models:

$$\sigma = -pI + \int_{\infty}^{t} \mu(t-t'; II_B(t'))[(1+\varepsilon)B(t,t') + \varepsilon C(t-t')]dt',$$

where σ is a deviatoric stress tensor; p is isotropic pressure; I is a unit tensor;

$$\mu(t-t'; II_B(t')) = \int_{-\infty}^{\infty} H(\theta)f(\theta)II_B(t')\exp-\left\{\int_{t'}^{t} \varphi(\theta; II_B(t''))\theta^{-1}\, dt''\right\}d\ln\theta;$$

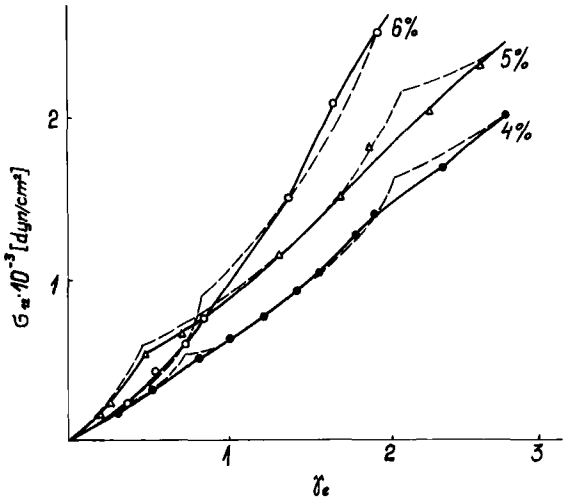

FIGURE 4 Relation $\sigma_{12} - \gamma_e$ for aqueous polyacrylamide solutions.[4] ——— experimental results; — — — — experimental results approximated according to Ref. 4.

$B(t,t')$ and $C(t,t')$ are Finger and Cauchy deformation tensors, respectively; II_B is the second invariant of the strain tensor; ε is a parameter characterising the first to second normal stress difference ratio; $H(\theta)$ is the relaxation time spectrum, $f(\theta; II_B(t))$ and $\varphi(\theta; II_B(t))$ denote modular and relaxation non-linearities, respectively. In the modular non-linearity case, $f(\theta; II_B(t)) \neq 1$, and $\varphi(\theta; II_B(t)) = 1$; in the relaxation non-linearity case, $f(\theta; II_B(t)) = 1$, and $\varphi(\theta; II_B(t)) \neq 1$; in the general non-linearity case, $f(\theta; II_B(t)) \neq 1$, and $\varphi(\theta; II_B(t)) \neq 1$.

2) Models:

$$\sigma = -pI + \int_{-\infty}^{t} \mu(t-t'; II_e(t'))[(1+\varepsilon)B(t,t') + \varepsilon C(t,t')]dt';$$

where

$$\mu(t-t'; II_e(t')) = \int_{-\infty}^{\infty} H(\theta) f(\theta; II_e(t') \exp -\left\{ \int_{t'}^{t} \varphi(\theta, II_e(t''))\theta^{-1}\, dt'' \right\} d \ln \theta;$$

$II_e(t)$ is the second invariant of the strain rate tensor, only if $f(\theta; II_e(t)) = 1$, and $\varphi(\theta; II_e(t)) \neq 1$.

3) Models:

$$\sigma = -pI + \int_{-\infty}^{t} G(t-t'; II_e(t'))[(1+\varepsilon)dB(t-t')/dt + \varepsilon\, dC(t,t')/dt']dt',$$

where

$$G(t-t'; II_e(t')) = \int_{-\infty}^{\infty} H(\theta) F(\theta, II_e(t')) \exp -\left\{ \int_{t'}^{t} \phi(\theta; II_e(t''))\theta^{-1}\, dt'' \right\} d \ln \theta,$$

only if $F(\theta; II_e(t')) \neq 1$ and $\phi(\theta; II_e(t'')) = 1$. For models 2 at $\varphi(\theta; II_e(t)) \neq 1$, and models 3 at $\phi(\theta; II_e(t'')) \neq 1$ as well as for corotational differential models, negative values of $G'(\omega, \dot{\gamma}_0)$ at $\omega \to 0$ should be observed at shear rates $\dot{\gamma}_0$ for which $d(P_{w1}/2\dot{\gamma})/d\dot{\gamma} > 0$. Figures 5 and 6 show our experimental results[7] and the experimental results by Booij[8] making evident that $\lim_{\omega \to 0} G'(\omega, \dot{\gamma}_0) < 0$ starting from $\dot{\gamma}_0$'s corresponding to $d(P_{w1}/2\dot{\gamma})/d\dot{\gamma} > 0$, i.e. starting from lower $\dot{\gamma}_0$'s as compared with those predicated according to Refs 5 and 6. Thus, the three experimentally observed phenomena, i.e. the melt squeezing out of the cone-and-plate assembly of the rheometer, eddy solution flows with irregular normal pressure oscillations, and negative values of the real component of the stationary flow solution response to an oscillatory shear, represent instability symptoms and are observed starting from those $\dot{\gamma}$ values at which $d^2E_e/d\dot{\gamma}^2 = 0$.

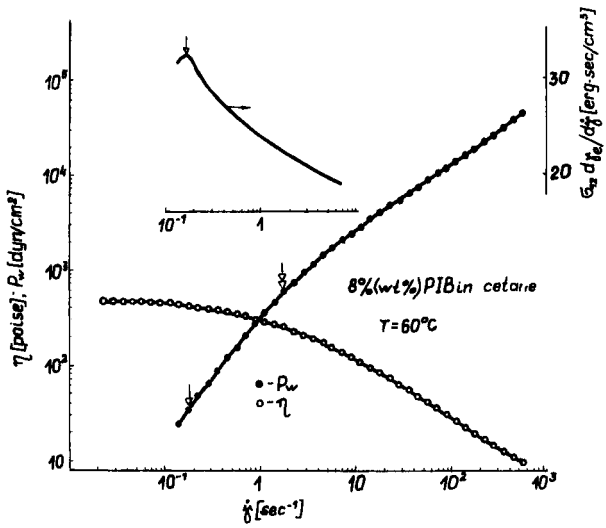

FIGURE 5 Eight per cent polyisobutylene solution in cetane.[7] ↓, experimentally determined lowest shear rate starting from which $\lim_{\omega \to 0} G'(\omega, \dot{\gamma}_0) \leqslant 0$; ↓, prediction according to Refs 5 and 6 of the lowest shear rate starting from which $\lim_{\omega \to 0} G'(\omega, \dot{\gamma}_0) \leqslant 0$.

2. LINEAR MONODISPERSE POLYMER MELT SHEAR FLOW STABILITY

Among recent advances made by the polymer melt rheology, of particular importance is the finding[9] that the steady flow of practically monodisperse linear polymers is described by linear viscoelasticity which is generalized to finite strains using the Jaumann differentiation operator, i.e. by a quasi-linear corotational model, such as

$$\sigma = \sum_{k=1}^{\infty} \sigma_k$$

$$\sigma_k + \theta_k \frac{D\sigma_k}{Dt} = -\eta_k \dot{\gamma}, \tag{4}$$

where σ is the stress tensor; $\dfrac{D\mathscr{C}_{ik}}{Dt} = \dfrac{\partial \mathscr{C}_{ik}}{\partial t} + v_j \dfrac{\partial \mathscr{C}_{ik}}{\partial x_j} + \omega_{ij}\mathscr{C}_{kj} + \omega_{kj}\mathscr{C}_{ij}$;

$$\omega \equiv \frac{1}{2}\left(\frac{\partial v_k}{\partial x_i} - \frac{\partial v_i}{\partial x_k}\right).$$

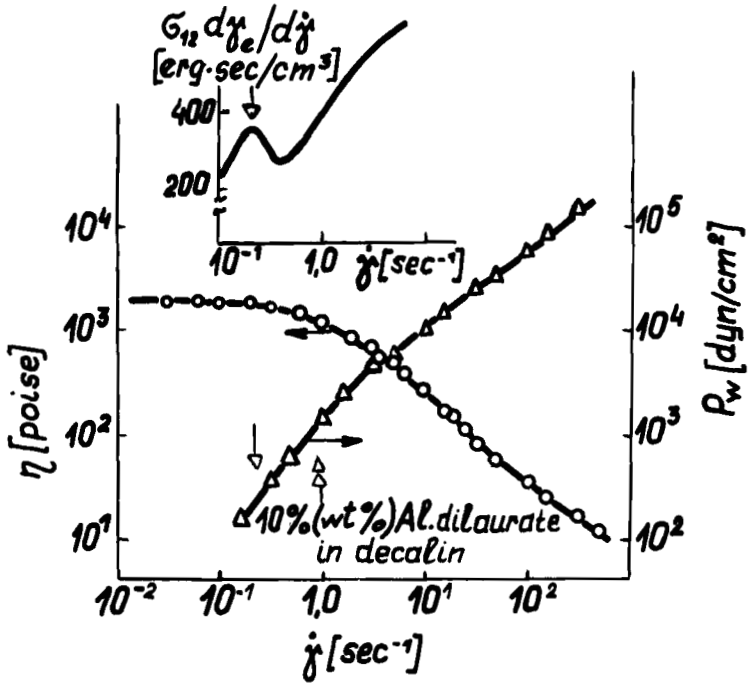

FIGURE 6 Ten per cent aluminium dilaurate solution in decalin.[8] ↓, experimentally determined lowest shear rate starting from which $\lim_{\omega \to 0} G'(\omega, \gamma_0 \leqslant 0$; ↑, prediction according to Refs 5 and 6 of the lowest shear rate starting from which $\lim_{\omega \to 0} G'(\omega, \dot{\gamma}_0) \leqslant 0$.

For the steady shear, it leads to $\eta = \sum_{k=1}^{\infty} [\eta_k/1 + \theta_k^2 \dot{\gamma}^2]$;

$$\kappa_1 = P_{w1}/2\dot{\gamma}^2 = \sum_{k=1}^{\infty} [\eta_k \theta_k/(1+\theta_k^2\dot{\gamma}^2)] = -2\kappa_2 = -P_{w2}/\dot{\gamma}^2$$

where $P_{w2} = \sigma_{22} - \sigma_{33}$. For the steady elongational flow, the elongation viscosity is

$$\lambda = 3\eta_0 \neq f(\dot{\varepsilon}), \qquad \dot{\varepsilon} = \ln(l/l_0)/t,$$

where $\eta_0 = \lim_{\dot{\gamma} \to 0} \sigma_{12}/\dot{\gamma}$. For monodisperse polymers and the above model for the steady shear flow, the following correlations hold true:

$$G''(\omega) = \sigma_{12}(\dot{\gamma});$$

$$2G'(\omega) = P_{w1}(\dot{\gamma}),$$

provided $\dot{\gamma} = \omega$. Here, it is possible to predict material functions $\eta(\dot{\gamma})$, $\kappa_1(\dot{\gamma})$ and $\kappa_2(\dot{\gamma})$ on the basis of linear visco-elastic function measurement results.

For this purpose, let us make use of the Zarembo–Fromm–DeVitt (ZFD) model,[10] the relaxation time spectra calculated according to the models by Marvin[11] and Graessley,[12] and the experimental data for frequency relations of the complex modulus components of linear narrow MWD polymers.[13–15] The results are listed in the table. The table shows that, for monodisperse polymers, the prediction is close to the experimental results. Note that, according to our experimental findings, $P_{w2} \approx -\frac{1}{2}P_{w1}$ for linear narrow MWD polymers, such as polybutadiene.

3. ELASTIC TURBULENCE OF MELTS FORCED THROUGH A NOZZLE

This occurs at extremely low Reynolds number values, when no inertial turbulence takes place. Elastic turbulence origination is localized

a) inside the nozzle—for linear polymer melt flows;

b) at the reservoir outlet to the nozzle—for long-chain macromolecular branching polymer flows.

There are certain indications that localized elastic turbulence origination depends both on the macromolecular structure and the MWD of the polymer.

For linear polymer melts, it is shown[17] that, starting from a definite flow rate, an extrudate with a rough surface is extruded, which then becomes smooth again. The analysis of the results obtained with various nozzle diameters suggests a conclusion that, in the latter case, there occurs a core flow with an approximately 0.02 mm thick wall layer of a low viscosity fluid. The dry friction hypothesis is to be rejected. The above effects may be explained using the polymer cluster flow hypothesis.[18] There should be suggested polymer melt segregation by fractions into clusters in a sequence which is a function of the shear rate: larger MW fractions change into clusters at low shear rates, with progressively lower MW fractions incorporated into clusters with increasing shear rate; clusters migrate from the nozzle wall towards the nozzle axis, and the wall layer is depleted by the high MW portion of the MWD, which fact is evidenced by numerous experimental findings. Cluster flow occurs within the steady shear flow starting from those shear rates which correspond to $d^2E_e/d\dot{\gamma}^2 < 0$.

In practically monodisperse linear polymers, the MW segregation is impossible; therefore, there is no core flow zone, and transition to the cluster flow is accompanied by continuity breaks.

The instability originating at the reservoir outlet to the nozzle should be

TABLE I

Critical parameters for steady shear flows of monodisperse polymers

No.	$\frac{\sigma_{12(k1)}}{\sigma_{12(k2)}}$	$\frac{\sigma_{12(k1)}}{\sigma_{12(k2)}}$	$\gamma_{e(k1)}$	$\gamma_{e(k2)}$	$\frac{\gamma_{e(k2)}}{\gamma_{e(k1)}}$	$\frac{\eta_{k1}}{\eta_0}$	$\frac{\eta_{k2}}{\eta_0}$	$\frac{\eta_{k2}}{\eta_{k1}}$
1. ZFD model[10] [a]	1.0/0.87	1.0/1.73	1.0/0.58	1.0/1.0	1.0/1.72	0.5/0.75	0.5/0.5	1.0/0.67
2. Model[11]	0.82	2.4	0.65	1.25	1.43	0.64	0.34	0.53
3. Model[12]	0.88	1.66	0.75	1.20	1.60	0.56	0.35	0.625
4. Polybutadiene[13]	0.69	5.0	0.6	1.4	2.33	0.56	0.146	0.258
5. Polystyrene[14]	0.65	4.85	0.65	1.45	2.33	0.61	0.221	0.362
6. Polystyrene[15]	0.60	6.4	0.58	1.4	2.40	0.61	0.207	0.340
7. Polybutadiene[16] [b]	$\sigma_{12(k)}/\sigma_{12(s)} = 0.83$	$\dot{\gamma}_s/\dot{\gamma}_k = 3.16$	—	—	—	$\eta_k/\eta_0 = 0.6$	—	—

[a] The numerator includes the value corresponding to $d^2E_e/d\dot{\gamma}^2 = 0$. In the denominator index k_1 is assigned to the values of $\sigma_{12}, \dot{\gamma}^*, \dot{\gamma}$ at corresponding to $d^2E_e/d\gamma_e^2 = 0$.

[b] Refers to stationary flow in a capillary voscosimeter; $\dot{\gamma}_k, \eta_k, \sigma_{12(k)}$ correspond to a "spurt" notion; $\sigma_{12(s)}$ is the stress at shear rate $\gamma_s = \omega_{max}$.[16]

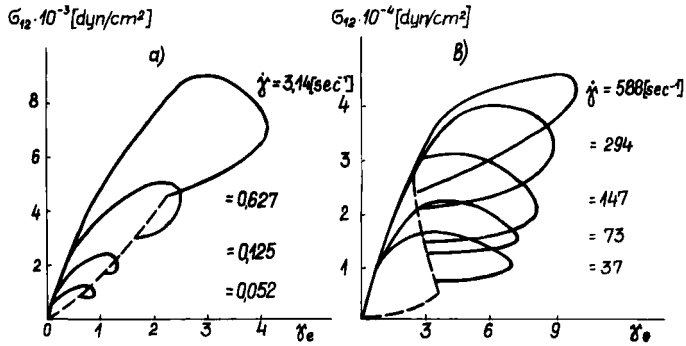

FIGURE 7 σ_{12} *vs.* γ_e relation for the pre-stationary flow with $\dot{\gamma}(t)$ specified by the step function for a) 15% polysobutylene PIB-200 solution in toluene;[8] b) same as above, for 20% polysobutylene solution in o-xylol.[19]

analysed by giving consideration to the prestationary flow within the reservoir-nozzle transition zone. Since the shear rate at the wall is proportional to the cubed radius, the shear rate in the reservoir may be equalized to zero as a first approximation. The further simplification is associated with the assumption of a step shear rate change from zero to the design steady value. For even further simplification purposes, let us consider Eq. (4) at $k = 1$.

This model represents the effects observed experimentally for $\sigma_{12}(\gamma_e)$ relations within the pre-stationary zone[19,20] at the shear rate specified by an approximately step function (Figures 7 and 8). Figure 9 shows viscosity $\eta = \sigma_{12}/(\dot{\gamma} - \dot{\gamma}_e)$ changes with time under the same deformation conditions for the ZFD model; these changes by their nature follow the experimental results[19] for polyisobutylene (Figure 10), with no recourse to the structural failure concept for explication of the results obtained.

Let us also consider the process of the G_0-normalized elastic energy E_e accumulation as a function of the accumulated strain γ_e at step-specified dimensionless shear rates $\theta\dot{\gamma}$ (Figure 11). The broken line here represents the steady flow regime. It is interesting to note, that, if $\theta\dot{\gamma} < 0.5$, then the $E_e(\gamma_e)$ function is increasing monotonously until the steady values are attained. At $\theta\dot{\gamma} \geqslant 0.5$, the E_e values ascend at first, and then descend, with an inflection (max $dE_e/d\gamma_e$ at $\gamma_e = \theta\dot{\gamma}$) formed in the ascending leg. Note that $P_{w1}/2\sigma_{12} = \gamma_e$ only when $t/\theta \to \infty$.

As shown in Refs 21 and 22, if the strain disturbance is specified with a step function so that the stress pulse amplitude values are equal to σ_{12} in the steady flow regime, a stability loss occurs at $\theta\dot{\gamma} \approx 0.45$. If $\theta\, d\dot{\gamma}/dt \to 0$, the $(\dot{\gamma}\theta)^*$ values are two times those obtained with $\dot{\gamma}\theta$ specified by the step function. However, with the step specification, $\dot{\gamma}\theta > 0.45$, stability loss does not occur instan-

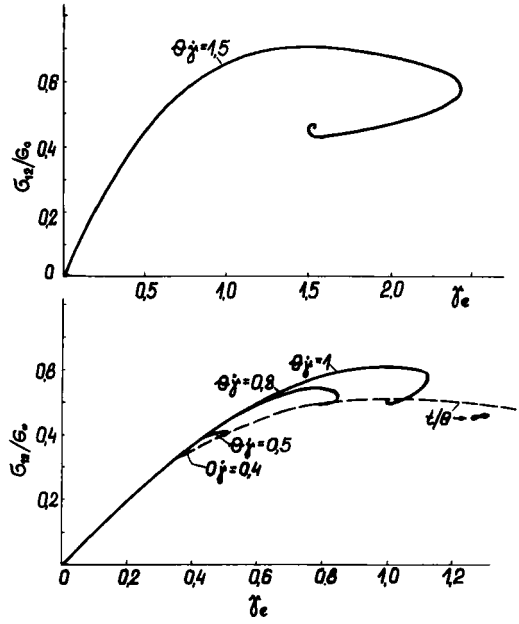

FIGURE 8 σ_{12} *vs.* γ_e relation for the pre-stationary flow according to the ZFD model with $\dot{\gamma}(t)$ specified by the step function for different $\dot{\gamma}\theta$ values indicated on the curves.

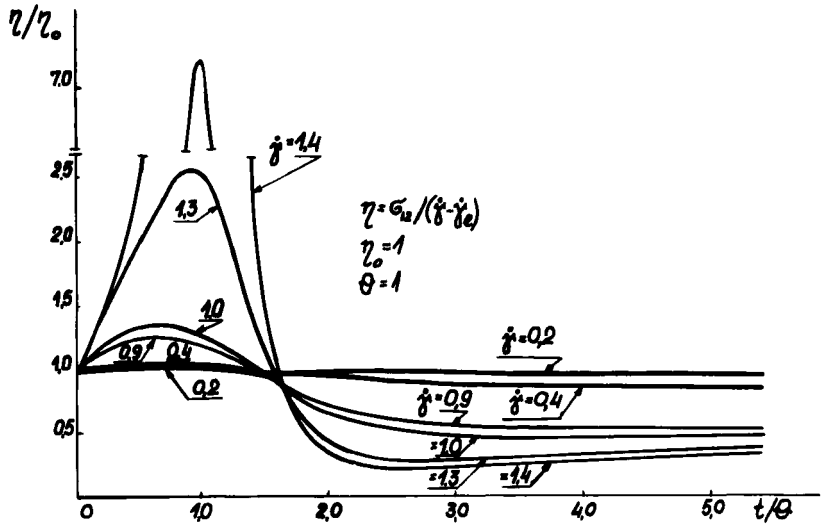

FIGURE 9 Kinetics of viscosity changes according to the ZFD model at shear rates as indicated.

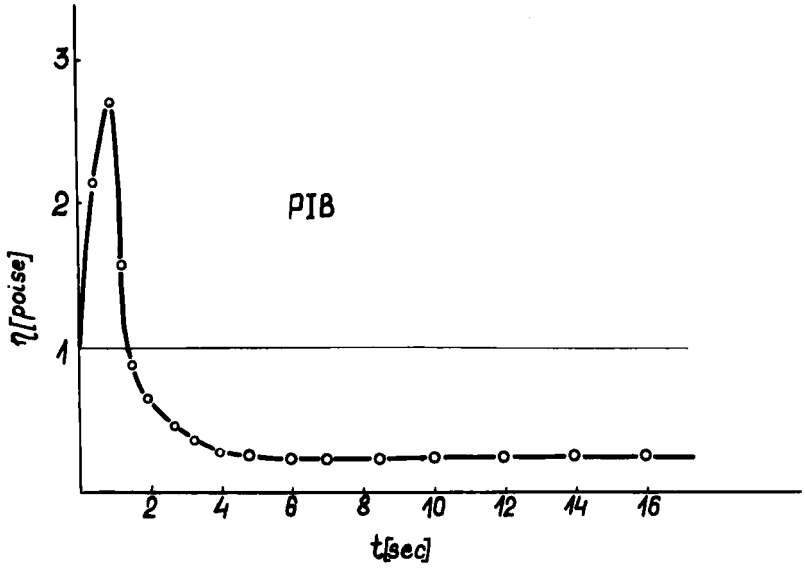

FIGURE 10 Same as in Figure 9, for polyisobutylene according to Ref. 18.

taneously, and the steady flow lasts for some time. The higher the $\dot{\gamma}\theta$, the lower the $(t/\theta)^*$. At shear rates $\dot{\gamma}\theta \approx 2.0$, the design reversible strain changes the sign at certain t/θ; in the Poiseuille flow case, this occurs near the capillary wall. In Ref. 23, this phenomenon is interpreted as a "hydrodynamic incompatibility" which leads to a stability loss.

In modern rotational instruments equipped with magnetic clutches, the duration of specified $\dot{\gamma}$ occurrences amounts to hundredth and thousandth fractions of a second. In capillary instruments, the duration of specified $\dot{\gamma}$ achievement is always incommensurably longer (when transferred from the reservoir into the capillary, the melt passes through a "funnel", the same stress states in the capillary cross-sections occur at a considerable distance from the inlet, etc.). This seems to be one of the causes for the flow instability to occur in the capillary rheometers at higher $\dot{\gamma}$ values, than in the rotational rheometers.

Thus, positivity of the second shear rate derivative of the elastic energy predetermines a possibility of steady polymer melt flow occurrences within a homogenous stress and strain rate field, as well as eddy solution flow occurrences. The same criterion predetermines a stable Poiseuille flow of linear polymers monodisperse by their MWs. When involved in the Poiseuille flow, polymers which are polydisperse by their MWs may get segregated by their fractions, if the elastic turbulence origination is localised within the

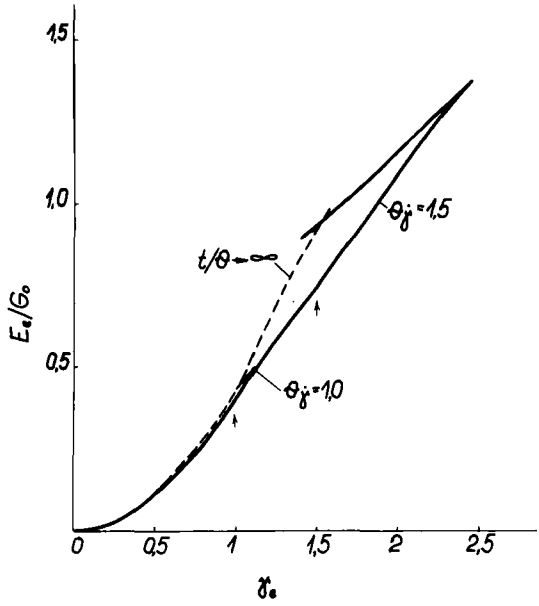

FIGURE 11 Specific elastic energy accumulation in the pre-stationary flow zone according to the ZFD model.

capillary. If the elastic turbulence origination is localised at the capillary inlet, then the pre-stationary deformation regimes should be analysed.

The cluster flow and one of its trends (eddy flow) should be regarded as an occurrence of a locally steady-state dissipative structure according to Prigozhin,[24] with the cluster origination and development conditions being related to polymer MWD. Polymer melt thixotropy is related to differences in characteristic times of cluster formation and disintegration.

With no cluster flow, there are no thixotropic events either. It is evident that the polymer solution and melt flows until cluster formation may be described by an appropriate geometrically non-linear phenomenologic rheological model, while a cluster flow should incorporate some physical non-linearity which indirectly accounts for the melt or solution transition from the homogenous fluid category to the inhomogenous fluid category.

References

1. L. A. Faitelson and I. P. Briedis, *Mekhanika Polimerov* **4**, 718 (1976).
2. R. G. King, *Rheologica Acta* **5**, 35 (1966).
3. W. M. Kulicke, H. E. Jeberien, H. Kiss and R. S. Porter, *Rheologica Acta* **18**, 711 (1979).

4. W. M. Kulicke and R. S. Porter, *J. Appl. Pol. Sci.* **23,** 953 (1979).
5. B. A. Bernstein, *Rheologica Acta* **11,** 210 (1972).
6. M. G. Ciprin and L. A. Faitelson, *Mekhanika Polimerov* 913 (1970).
7. L. A. Faitelson and E. E. Jakobson, *Mekhanika Kompozitnykh Materialov* **2** (1981).
8. R. S. Booij, Ph.D. Thesis Leiden, 126 p. (1970).
9. F. V. Vinogradov, *Mekhanika Polimerov* **6,** 1062 (1977).
10. R. B. Bird, R. C. Armstrong and O. Hassager, *Dynamics of polymeric Liquids* (John Wiley and Sons, 1976), 727 p.
11. R. S. Marvin, in: J. I. Bergen, *Viscoelasticity—Phenomenological Aspects* (N.Y., 1960), p. 27.
12. W. W. Graessley, *J. Chem. Phys.* **54,** 5143 (1971).
13. G. Marin, *These Dr. Sci. Academie de Bordeux* (1977), 258 pp.
14. V. V. Barantshejeva, *These Dr. Sci.* (Moskva, 1977).
15. S. Onogi, T. Masuda and K. Kitagawa, *Macromolecules* **3,** 109–25 (1970).
16. G. V. Vinogradov, Flow High Elasticity and Relaxation Characteristics of Polymer Systems. Lecture in Seminar. (Hercog-Novi, Yugoslavia, 1970), 44 pp.
17. E. Uland, *Rheologica Acta* **18,** 1 (1979).
18. W. F. Busse, *J. Polymer Sci.* A-2, **5,** 1261 (1967).
19. A. Ya. Malkin, B. V. Yarlykov and G. V. Vinogradov, in: *Uspechi Rheologii Polimerov,* (Moskva, *Chimiya* 1970), 206–28.
20. A. A. Trapeznikov, in: *Uspechi Kolloidnoj Chimii* (Moskva, *Nauka,* 1973), 201–11.
21. V. N. Burlii and L. A. Faitelson, Soobščenije na 11 Vsesojuznom Simpoziume po reologii, Suzdal, 1980.
22. V. N. Burlii, in: *Vtoraya konferenciya molodih specialistov po mekhanike kompozitnikh materialov,* (Riga, *Zinatne,* 1979), pp. 61–62.
23. I. L. White, *J. Appl. Polym. Sci.* **8,** 1129 (1964).
24. W. Ebeling, *Strukturbildung bei Irreversiblen Prozessen* (Taubner Verlagsgesellschaft, 1976).